Hydrological Sciences Journal
Publication details, including instructions for authors and subscription information:
http://www.tandfonline.com/loi/thsj20

Evidence of groundwater flow on Antizana ice-covered volcano, Ecuador / Mise en évidence d'écoulements souterrains sur le volcan englacé Antizana, Equateur

VINCENT FAVIER [a] [b] , ANNE COUDRAIN [b] , ERIC CADIER [c] , BERNARD FRANCOU [c] , EDGAR AYABACA [d] , LUIS MAISINCHO [e] , ESTELLE PRADERIO [a] [f] , MARCOS VILLACIS [b] & PATRICK WAGNON [g]

[a] CEAZA , Benavente 980, casilla 599, La Serena, Chile E-mail:

[b] IRD, Great Ice (UR IRD R032), Maison des Sciences de l'Eau , BP 64501, 34394, Montpellier Cedex 5, France

[c] IRD, Great Ice (UR IRD R032) , Whymper 442 y Coruña, Casilla 17-12-857, Quito, Ecuador

[d] EMAAP-Q , Av. Mariana de Jesus y Alemania, Quito, Ecuador

[e] INAMHI , Iñaquito 700 y Corea, Quito, Ecuador

[f] Hydrétudes , 815, Route de Champ Farçon, 74370, Argonay, France

[g] IRD, Great Ice (UR IRD R032) , LGGE, 54 rue Molière, BP 96, 38402, Saint Martin d'Hères, France

Published online: 18 Jan 2010.

Evidence of groundwater flow on Antizana ice-covered volcano, Ecuador

VINCENT FAVIER[1,2], ANNE COUDRAIN[2], ERIC CADIER[3], BERNARD FRANCOU[3], EDGAR AYABACA[4], LUIS MAISINCHO[5], ESTELLE PRADERIO[1,6], MARCOS VILLACIS[2] & PATRICK WAGNON[7]

1 *CEAZA, Benavente 980, casilla 599, La Serena, Chile*
vifavier@gmail.com
2 *IRD, Great Ice (UR IRD R032), Maison des Sciences de l'Eau, BP 64501, 34394 Montpellier, Cedex 5, France*
3 *IRD, Great Ice (UR IRD R032), Whymper 442 y Coruña, Casilla 17-12-857, Quito, Ecuador*
4 *EMAAP-Q, Av. Mariana de Jesus y Alemania, Quito, Ecuador*
5 *INAMHI, Iñaquito 700 y Corea, Quito, Ecuador*
6 *Hydrétudes, 815, Route de Champ Farçon - 74370 Argonay, France*
7 *IRD, Great Ice (UR IRD R032), LGGE, 54 rue Molière, BP 96, 38402 Saint Martin d'Hères, France*

Abstract Hydrological and glaciological data were gathered in the watershed (1.37 km^2) of the Antizana Glacier 15 (0.7 km^2) in the periods 1997–2002 and 1995–2005, respectively. In addition, tracer experiments were carried out to analyse the flow through permeable morainic deposits located between the glacier snout and the runoff gauging station. Over 11 years, the mean specific net balance of the glacier was negative (–627 mm w.e.), despite the occurrence of positive values in the La Niña years (1999–2000). From the glacier net mass balance between 1997 and 2002, it was found that the mean flow originating from ice melt was significantly higher than the mean discharge measured at the hydrological station. Analyses of tracer experiments and of the different components of the hydrological balance suggest groundwater flow that originates below the glacier accounts for the remaining water. This result is important for regional analyses of available water resources and for the relationship between hydro-cryospheric processes and volcanic activity.

Key words Ecuador; hydrological balance; tracer experiments; tropical glaciers; groundwater flow; water resources

Mise en évidence d'écoulements souterrains sur le volcan englacé Antizana, Equateur

Résumé Des mesures hydrologiques (1997-2002) et glaciologiques (1995–2005) ont été effectuées sur le bassin versant (1.37 km^2) du glacier 15 de l'Antizana (0.7 km^2). Parallèlement, des essais de traçage ont été réalisés afin d'analyser les écoulements au travers des dépôts morainiques situés entre le front du glacier et la station hydrologique. En onze ans, le bilan de masse spécifique moyen du glacier est négatif (–627 mm eq.e) malgré les bilans positifs observés au cours de La Niña de 1999–2000. Entre 1997 et 2002, le débit moyen de fonte évalué à partir des données glaciologiques est supérieur au débit moyen mesuré en aval de la moraine. L'analyse des essais de traçage et des termes du bilan hydrologique indique que cette différence provient d'écoulements souterrains sous le glacier. Ce résultat est important pour évaluer les ressources en eau disponibles à l'échelle régionale et analyser la relation entre les processus hydrologiques et l'activité volcanique.

Mots clefs Equateur; bilan hydrologique; essais de traçage; glaciers tropicaux; écoulements souterrains; ressources en eau

INTRODUCTION

During the last 20 years, tropical glaciers have undergone considerable shrinkage (e.g. Ribstein *et al.*, 1995; Wagnon *et al.*, 1999; Francou *et al.*, 2000, 2004; Kaser & Osmaston, 2002; Coudrain *et al.*, 2005; Sicart *et al.*, 2005). The peculiar hydrological characteristics of glacierized catchments make them of special interest for water supply. In particular, precipitation is stored as snow and ice, and its contribution to streams is thus delayed. In moderately glacierized watersheds, glaciers reduce flow variability by sustaining discharge during periods of low precipitation (e.g. Fountain & Tagborn, 1985; Ribstein *et al.*, 1995; Kaser *et al.*, 2003a). This situation is particularly interesting at low latitudes because ablation occurs all year round and melting never completely stops (in contrast to the difference between winter/summer melting in mid- and high-latitude catchments (e.g. Kaser & Osmaston, 2002)). This flow stability is highly exploited in the Andes by water management industries, e.g. in the Zongo valley near La Paz (Bolivia) (Caballero *et*

Open for discussion until 1 August 2008

al., 2004) and in the Cañon del Pato (Callejon de Huaylas) in Peru (Kaser *et al*., 2003a; Pouyaud *et al*., 2005). This is also the case in Ecuador, even though Ecuadorian glaciers represent an area of only 90 km^2 (Kaser & Ostmaton, 2002). Due to the increasing demand for water, an important recollection project is planned in high-altitude areas to supply water to Quito and to the inter-Andean plateau (*Proyecto Ríos Orientales*) with a mean exploitation flow of 20.45 m^3 s^{-1} and hydro-electric production of 172 MW. This is an extension of the existing high altitude water recollection network with a water supply from La Mica of about 2.05 m^3 s^{-1} and hydro electric production of 9.5 MW (EMAAP-Q, 2002, pp.7). In this context, it is particularly important to study hydro-cryospheric processes and the impact of the rapid shrinkage of the glaciers on water resources in this region.

In Ecuador, glaciers only exist above 4800 m a.s.l. These altitudes are only encountered in volcanic ranges, and major Ecuadorian ice bodies cover stratovolcanoes, such as Chimborazo, Cotopaxi, Cayambe and Antizana (Hastenrath, 1981). Our study focused on Antizana volcano, which is located 40 km southeast of Quito and where glaciological, hydrological and meteorological programmes were established to study climate/glacier relationships and water resources from the cryosphere (e.g. Francou *et al*. 2000, 2004; Favier *et al*., 2004a,b; Cadier *et al*., 2007).

In this paper, after a general description of the study site, we successively present the basic glaciological and hydrological equations and data used in the study. The following section focuses on the comparative analyses of hydrological and glaciological measurements. We describe tracer experiments performed to estimate the groundwater flows in the catchment and then we highlight the possible interactions between groundwater flow and volcanic activity. In the last section, we discuss the contribution of water from glaciers to lower-altitude discharges and draw a number of conclusions.

DESCRIPTION OF THE STUDY SITE

Antizana (0°28′S, 78°09′W) is an ice-covered stratovolcano in the eastern Cordillera of Ecuador. The study area belongs to the inner tropics (e.g. Kaser, 2001) where temperature and humidity display low temporal variability throughout the year and, as a consequence, accumulation and ablation occur simultaneously almost all year round.

Hydrological, glaciological and meteorological measurements began in 1994 on Antizana Glacier 15 (Fig. 1) in the framework of a research programme conducted by the Great Ice research unit of IRD (French Research Institute for Development) in collaboration with INAMHI (*Instituto NAcional de Meteorología e HIdrología*) and EMAAP-Q (*Empresa Metropolitana de Alcantarillado y Agua Potable de Quito*). The study site is a remarkably well constrained catchment, which makes it well suited to investigation. Antizana Glacier 15 is a reference site of the long-term ORE-Glacioclim observatory (Francou *et al*., 2000, 2004; Favier *et al*., 2004a,b); it has two similarly oriented side-by-side snouts, called Glacier 15α and Glacier 15β, that extend from 5760 m a.s.l. down to 4840 m a.s.l. It is located on the NW slope of Antizana volcano (Fig. 1). Below the glacier snouts, the two main surface streams flowing from Glacier 15α and Glacier 15β disappear at 4780 m a.s.l. (labelled point D in Figs 1 and 2) upstream from a large moraine that was probably last active in 1950. Downstream from the moraine, about 50 m below point D, several springs feed the bed of the single surface stream that flows towards Limni 15 hydrometric station (referred to as Limni 15 Station hereafter) which is located at 4550 m a.s.l. The 1950 moraine is made of heterogeneous material, including sands and stones, and is hence quite permeable. It also includes dead ice, the progressive melt of which induces modifications in the terrain with surface collapse and changes in location of the springs. For instance, collapse allowed the formation of a small lake on the upstream slope of the moraine between 2000 and 2003 (Fig. 2). Other diffuse springs located between 4750 m a.s.l. and 4550 m a.s.l. contribute to the runoff measured at Limni 15 Station. Their flow is continuous with weak diurnal variations. Observation of minimal nocturnal discharges enabled estimation of their contributions which ranged from 2 to 5 L s^{-1}.

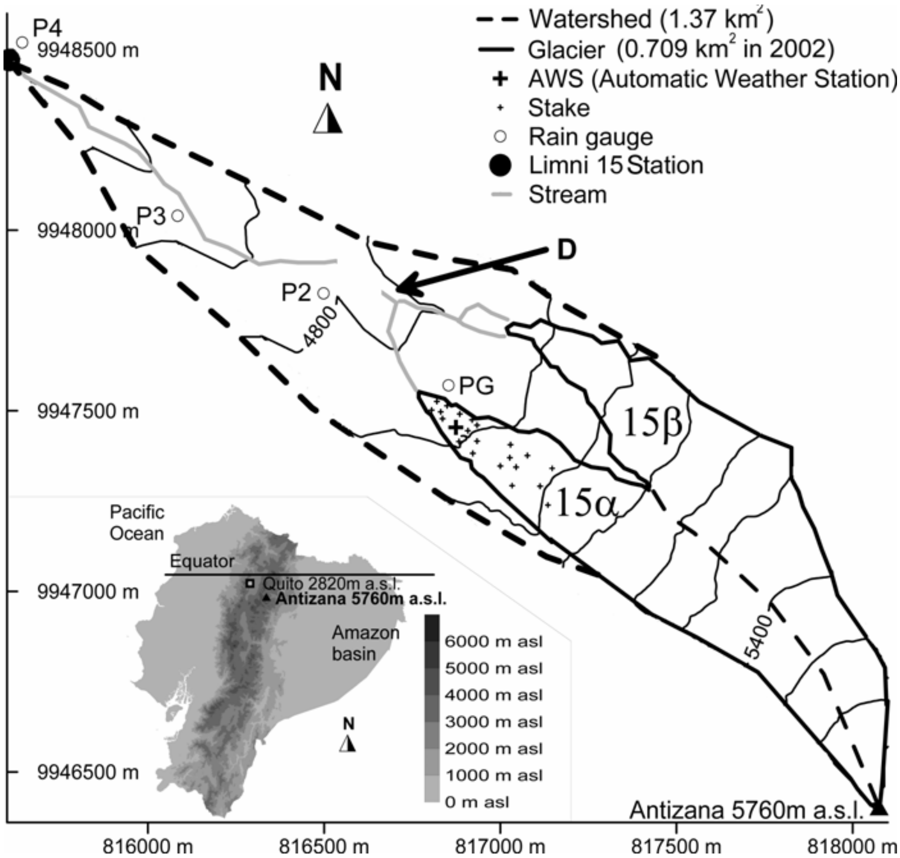

Fig. 1 Orientation map of Ecuador (lower left corner) and of Antizana Glacier 15 watershed and glacier. Monitoring equipment installed in the area and observed surface streams are also shown. Projection is on UTM zone 17.

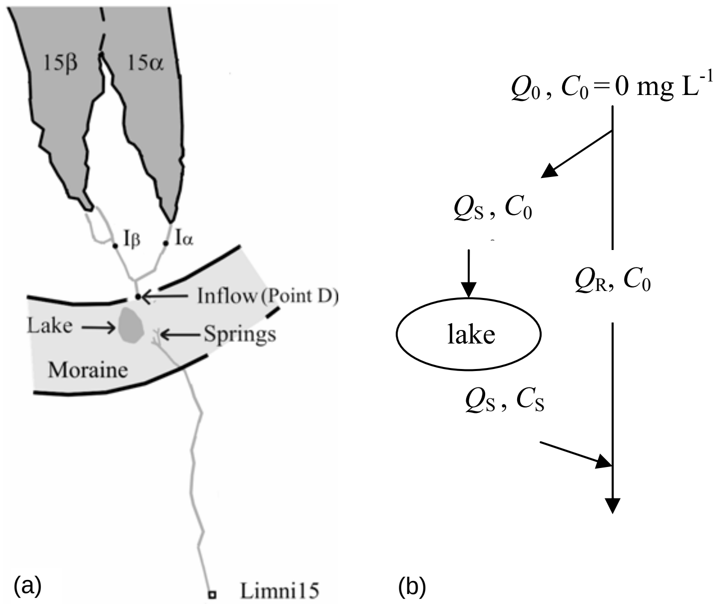

Fig. 2 Map (a) and schematic diagram (b) of observed surface streams at the level of the frontal moraine. The distribution of glacier meltwater discharge (Q_0) with (C_0) tracer salt into a slow circulation (Q_S) and into a rapid circulation (Q_R) is also shown. Water from the lake infiltrates or flows out with tracer salt (C_S) and finally mixes with rapid circulations.

THEORY AND EQUATIONS

The following subsections present annual specific mass balance over glacierized areas and the hydrological budget of the whole catchment.

Glaciological balance and melting term

The annual glaciological specific mass balance (B_n) was computed for the glacierized area, including the two snouts 15α and 15β, whose surface area ranged between 0.794 km^2 in 2000 and 0.620 km^2 in 2005. Annual values of B_n were estimated on the basis of the stake measurements made in the accumulation and ablation areas; the equation of annual specific mass balance enabled computation of the melting term LF_n through the following equation:

$$B_n = P_n - S_n - LF_n \text{ (mm w.e. year}^{-1}) \quad (1)$$

where P_n corresponds to precipitation, and S_n is the sublimation term. In this equation, melting induced by friction (potential energy loss due to glacier motion) and by the geothermal heat flux is assumed negligible.

Hydrological balance

The hydrological balance was computed for the whole catchment corresponding to Limni 15 Station (1.37 km^2), including the glacierized and non-glacierized areas (Fig. 1). With A_{ug} the non-glacierized area, the annual mass balance can be expressed by:

$$Q_n = Q_{glacier} + Q_{di} + P_n \times A_{ug} - \text{ETR} \times A_{ug} - Q_{gw} \text{ (m}^3 \text{ s}^{-1}) \quad (2)$$

where Q_n is the discharge at Limni 15 Station; $Q_{glacier}$ is equal to LF_n multiplied by A_g the surface of glacierized area, Q_{di} is the flow originating from melting at the bedrock–glacier interface and from melting of the dead ice located in the non-glacierized area; P_n is precipitation assumed constant over the whole catchment (cf. justification below in the text); ETR is evapotranspiration from the non-glacierized area and Q_{gw} corresponds to possible outflow from the catchment by groundwater flow; this flow would originate either from the glacierized or from the non-glacierized areas.

However, Q_{di} values are difficult to assess; a rough computation of the energy loss from glacier motion allows estimation of melt equal to about 0.5 L s^{-1}. Estimating that melting of dead ice may produce a similar discharge value, Q_{di} is assumed equal to 1 L s^{-1}.

Equation (2) shows that if groundwater flow is negligible, as assumed for instance in previous studies in Peru or Bolivia (e.g. Pouyaud *et al*., 2005; Sicart *et al*., 2007), and evapotranspiration is assumed to be lower than precipitation, Q_n values should be higher than $Q_{glacier}$ values.

MEASUREMENT PROGRAMME

Glaciological data

The glaciological data used in this study are the following:

– Monthly ablation measurements of Antizana Glacier 15 from January 1997 to March 2003;
– Annual specific mass balance (B_n) on Antizana Glacier 15 from 1995 to 2005.

The glaciological measurements and methods we used have already been presented by Francou *et al*. (2004). The monthly measurements of ablation stakes were made at the beginning of each month in the ablation zone between 5050 and 4840 m a.s.l., where each elevation range of 50 m contained a minimum of four ablation stakes. When snow was present on the ice, its depth was measured within a 1-m radius around the stake. Snow density was assumed equal to the value generally estimated (ρ = 400 kg m^{-3}) because of its low variability. To process the net specific balance, we divided the ablation zone into elevation ranges of 30–50 m and performed homogeneity tests between all the stakes in one elevation range to eliminate non-representative points. Because precipitation generally increases slightly in January and decreases slightly in June, the hydrological year in this part of Ecuador was set to coincide with the calendar year, from 1 January to 31 December. The specific net balance of the entire glacier was estimated every year by integrating net accumulation measurements made at the beginning of the hydrological year in the upper glacier zone, allowing assessment of the mass balance value (Table 1). Each year, accumulation was obtained from snow pits excavated at two or three locations and from various snow depth measurements from probing, in accordance with UNESCO mass balance protocols (e.g. Kaser *et al.*, 2003b; Francou & Pouyaud, 2004). Mass balance measurements have an uncertainty of ±400 mm w.e. in the accumulation area (e.g. Sicart *et al.*, 2007) and ±100 mm w.e. in the ablation area.

Table 1 Comparison between hydrological and glaciological data of Antizana Glacier 15 (1995–2005).

	1997	1998	1999	2000	2001	2002	Mean (1997–2002)	Mean (1995–2005)
1. Specific net mass balance, B_n (mm w.e. year^{-1})	–612	–845	515	393	–598	–769	–319	–627
2. Annual sublimation, S_n (mm w.e. year^{-1})	–377	–399	–380	–380	–356	–300	–365	–362
3. Annual Precipitation[(a)], P_n (mm year^{-1})	930	1374	1335	1215	910	985	1124	1020
4. Computed annual melt, LF_n (mm w.e. year^{-1})	1165	1819	440	442	1152	1454	1079	1285
5. Production coefficient of the glacierized area (LF_n/P_n)	1.25	1.32	0.33	0.36	1.27	1.48	0.96	1.26
6. Surface of glaciers 15α and 15β, A_g (km^2)	0.747	0.737	0.750	0.794	0.758	0.709	0.749	0.725
7. Computed potential annual discharge from melt water,	27.6	42.5	10.5	11.1	27.7	32.7	25.4	29.2
8. Measured annual discharge at Limni 15 station, Q_n (L s^{-1})	25.5	25.6	11.4	10.7	11.8	14.2	16.5	
9. ETR × A_{ug} + Q_{gw} (L s^{-1})[(b)]	21	45	26	24	35	40	32	
10. Q_{gw} (L s^{-1}) assuming ETR = 362 mm year^{-1}	14	38	19	17	28	33	25	
11. Q_{gw} (L s^{-1}) assuming ETR = 850 mm year^{-1}	5	28	10	8	18	22	16	
12. Production coefficient (Q_n/P_n) for 1.37 km^2	0.63	0.43	0.20	0.20	0.30	0.33	0.34	

[(a)] Precipitation was measured at 4650 m a.s.l.
[(b)] ETR is evapotranspiration from the non-glacierized area, A_{ug} is the surface of the non-glacierized area, and Q_{gw} corresponds to possible groundwater flow that would not reach Limni 15 station and could originate either in the glacierized or non-glacierized part of the catchment.

Use of reanalysed data to estimate sublimation

This section deals with the estimation of the sublimation term (S_n in equation (1)) for the period 1995–2005. Two methods were used, depending on the period.

From 14 March 2002 to 14 March 2003, the estimation is based on the computation of turbulent heat fluxes because for this specific period the meteorological data necessary for this computation were available (Favier *et al.*, 2004a,b). The method used, called the bulk method, approximates the turbulent heat fluxes from only one level of measurements over the soil surface (Arck & Scherer, 2002). It requires surface roughness lengths to be computed. Like in Wagnon *et al.* (1999), the surface roughness lengths were all chosen equal, and were used as single parameters that were calibrated from direct sublimation measurements performed with lysimeters during eight field trips of 5–9 days each. The accuracy of the estimation of the sublimation by this method is difficult to assess. However, a detailed study of the temperature and wind speed profiles in the first 5 m of the atmosphere showed that the meteorological measurements made at 2 m over the ice surface were within the dynamic sublayer. This allows the assumption that, in these conditions, the use of the bulk method is justified and leads to a limited uncertainty in the estimation of the sublimation.

For the period 1995–2005, except the period from 14 March 2002 to 14 March 2003, the estimation of the monthly sublimation term was based on monthly values of NCEP-NCAR reanalysis from the grid cell closest to Antizana (77.5°W, 0°S) at the 500 hPa level (around 5500 m a.s.l.) and on the use of an empirical relationship. This relation (see Francou *et al.*, 2004, for details) takes into account that the latent turbulent heat flux depends mainly on wind velocity and on humidity:

$$S_n = \alpha\,(q - q_s)\,v \text{ (mm w.e. month}^{-1}\text{)} \quad (3)$$

where q is mean monthly air specific humidity in (kg kg^{-1}); q_s is surface specific humidity in (kg kg^{-1}) for a snow/ice surface in melting conditions at 500 hPa; v is the monthly mean wind speed in (m s^{-1}); and α is a unit constant for homogeneity of equation (3). Even though the uncertainty on computed sublimation values is hard to assess, the validity of this equation was tested over the period from March 2002 to March 2003. The correlation between the S_n values computed by equation (3) and from computation of the turbulent latent heat flux at the glacier surface was high, $r = 0.78$, (significant at $p = 0.01$ level); see Fig. 7(a) in Francou *et al*. (2004). Moreover, the computed sublimation value for one year (315 mm w.e.) was almost equal to meteorological measurements made on the glacier itself (300 mm w.e.).

The monthly computed sublimation values for the whole 11-year period (1995–2005) were summed to assess annual sublimation (Table 1).

Hydrological measurements

In this study, the chronological series of hydrological data taken into account are those computed from the continuous series of data collected at Limni 15 Station (4550 m a.s.l.) and from the raingauge located at 4650 m a.s.l. on the Antizana Glacier 15 watershed:

– monthly discharge from December 1996, to March 2003;
– annual discharge from 1997 to 2002; and
– annual precipitation from 1995 to 2005.

The Limni 15 station collects the streams originating from the melting of Glaciers 15α and 15β. The station was built in December 1995, but several technical improvements were necessary, and measurements can only be considered as valid since December 1996. Considerable changes were made to the station during the study period to improve the quality of the measurements. The difficulties encountered were linked to the high variability of the discharge, which generally varies between 4 and 60 L s^{-1} each day, but which can vary between 2 and 200 L s^{-1} in less than 2 hours. The quantity of solids transported and deposition/erosion in the gauging channel also led to measurement problems. Moreover, on 20 August 1998, a big instantaneous flood destroyed the Limni 15 station and parts had to be rebuilt. Water depth in the gauging channel was measured every minute with a pressure gauge. The calibration curve of the station between water depth in the gauging channel and discharge was based on volumetric measurements. An uncertainty analysis was performed on the calibration curve because the scattering of the points obtained by volumetric measurements (height *vs* discharge) was not negligible. This allowed the computation of minimal and maximal possible discharges over the study period (Figs 3 and 4). Due to marked changes in discharge uncertainty over the study period, we considered two main periods (Favier, 2004):

From December 1996 to 27 March 2002, the actual annual flow value ranged between –60% and +90% around the estimated value. It was impossible to measure the volume of the flood that occurred on 20 August 1998, but as it only lasted a few minutes, its volume was clearly negligible compared to monthly and annual discharges and the flood was not taken into account in our computations.

From 27 March 2002 to March 2003, the quality of water depth measurements had improved and the final accuracy of discharge values was estimated to be ±25%.

Precipitation, P_n, was estimated from raingauge measurements. Three raingauges were installed between 4500 and 4860 m a.s.l. in the catchment and were measured during the 1995–2005 period (P2, P3 and P4 labels in Fig. 1). One more raingauge was installed in 2002 (PG at 4860 m a.s.l.). The annual precipitation from these different raingauges displays significant differences (around 20%) that are within the uncertainty range of the measurement equipment. Considering the altitude effect, opposite trends were found from one year to another (Favier, 2004). Mean precipitation at P2 is lower by 20% than on the other raingauges. This can be related to the occurrence of higher values of wind speed close to the moraine that presents important local

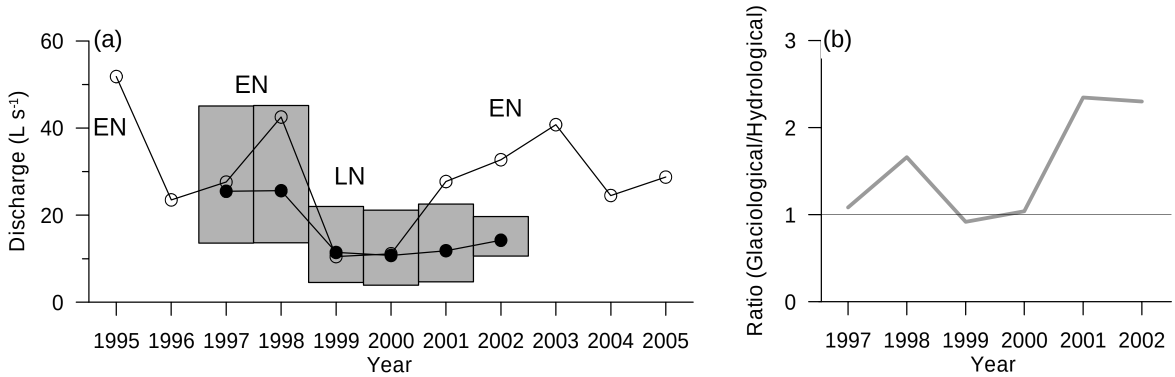

Fig. 3 (a) Comparison between mean annual discharge values at Limni 15 Station (solid circles), computed from water height measurements at the station and calibrated curves, and annual melt flow from Glacier 15 (glaciers 15α and 15β) (open circles), computed from the glaciological mass balance between 1995 and 2005. Grey rectangles represent the maximum uncertainty for discharge measurements. EN indicates an El Niño event, and LN a La Niña event. (b) Ratio between the annual estimated melting discharge from Glacier 15 and the annual measured discharge at Limni 15 station. The $y-1$ line is also shown.

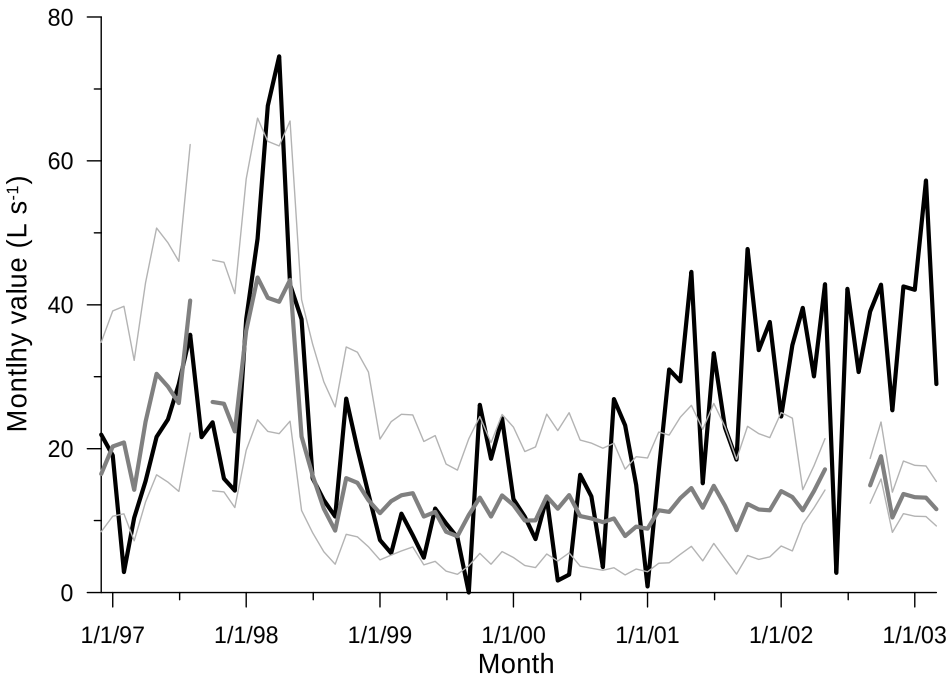

Fig. 4 Comparison between monthly discharges (thick grey line) measured at Limni 15 station and monthly melt values computed for the ablation area of Antizana Glacier 15 (between 4840 and 5050 m a.s.l.) (thick black line), from December 1996 to March 2003. Thin grey lines represent the maximum and minimum discharges taking into account a maximum possible range of error in measurements of the discharge at Limni 15 station.

relief. Raingauge P4 experienced some failures and data are sometimes questionable. Precipitation collected at Raingauge P3 (4650 m a.s.l.) is complete during the period under consideration, is coherent, and presents values close to the mean value computed with the data of the four raingauges when available. Due to the small size of the glacier and to the relatively good agreement between precipitation measurements from the different raingauges on the Antizana Glacier 15 catchment, as well as accumulation measurements performed at the summit, values registered at P3 were used as an estimation of the precipitation for the whole catchment area.

Tracer experiments

Tracer experiments (e.g. Collins, 1979) were performed to study flow paths through the 1950 moraine of Antizana Glacier 15 using NaCl solutions, as this salt can be assumed to be entirely conserved in solution (e.g. Sigg *et al.*, 1992). Small volumes (50–80 L) of brines with known quantities of salt (NaCl, see Table 2) were injected at specific points (for details, see below) upstream from the moraine. Downstream from the moraine, the electric conductivity (in S cm^{-1}) of the stream water was then measured at Limni 15 station. The relationship between conductivity and concentration was established for the specific conditions of each injection through measurements on water samples with different concentrations of salt. Conductivity values ranged from 6 µS cm^{-1} in the case of non-salted waters, to 700 µS cm^{-1} at maximum conductivity of waters containing the tracer salt. The restitution rates were computed with the Qtracer2© program, which was designed for analysis of tracer experiments.

Table 2 Results of tracer experiments performed in surface streams and in the small lake located on the moraine.

Day	Mean and maximum discharge[a] (L s^{-1})	Injected mass of salt (kg)	Restitution rate[b] (%)	Response time [c] (min)	Transfer time [b] (min)
18/12/2002	11.1 *(19.7)*[a]	20	21.3	175	276
16/01/2003	22.6 *(35)*	30	59.8	97	159
02/02/2003	1.8 *(3.7)*	24	5.8	288	394
26/02/2003	15.2 *(21.9)*	24	51.7	115	158
27/02/2003	22.5 *(34.8)*	20	58.2	98	125
21/05/2003	77.7 *(105.5)*	21.4	75.4	65	95
24/05/2003	86.3 *(104.7)*	17.8	68.8	52	72.3
10/06/2003	65.5 *(78)*	24	62.8	57	72.2
03/07/2003[d]		4.9	93[e]	420	

[a] Between conductivity increase and retrieval of the initial conductivity value. Maximum discharge values during each experiment are in italics.
[b] Computed with Qtracer2©.
[c] Time between injection and increase in conductivity.
[d] Injection of tracer in the lake.
[e] Restitution of the NaCl mass loss of 4.9 kg between 3 July at 14:00 h LT (injection time) and 5 July at 12:00 LT.

Eight experiments, hereafter referred to as “stream experiments”, were conducted by injecting brine solutions in surface streams flowing from the snouts of Glacier 15α and 15β upstream from the moraine at points Iα and Iβ, respectively (Table 2 and Fig. 2). Electric conductivity was then measured at Limni 15 Station until conductivity reached its initial value (after around 4 hours). Conductivity measurements were always performed around midnight and in the morning of the following day to check that no further increase in conductivity occurred. The time of injection was close to 14:00 h local time (LT) when discharge usually presents maximum diurnal values, and is relatively stable for a few hours. The mean discharges at Limni 15 station during these experiments ranged from 1.8 to 86.3 L s^{-1}. Another experiment (Table 2), called “lake tracer experiment”, was then conducted by injecting a brine solution into the lake located on the upstream slope of the moraine.

During tracer experiments, the discharge at the Limni 15 station was determined by water depth measurements (every minute) and by volumetric discharge measurements. For the first eight experiments, the volumetric discharge measurements were performed every 10 min for 5 h and every 5 min during the hour following the peak of conductivity. During the “lake tracer experiment”, discharges were measured once per hour for 3 days. Conductivity was measured with a WTW 340i conductimeter (accuracy of ±0.5 %). In the “stream experiments”, conductivity at Limni 15 station was measured every 2 min (and every 30 s during the hour following maximum salinity), whereas in the lake tracer experiment, conductivity was measured every 20 min for 3 days after injection.

During the course of the experiments, water temperature varied widely (from 0 to 18°C), and these changes were taken into account in the conductivity measurements (e.g. Lecce, 1993). The impact of temperature on conductivity values can be taken into account by applying a temperature correction coefficient b_T, whose value changes with mineralization. Field measurements showed that b_T values ranged between 0.026°C^{-1} in water with no added NaCl solution and ~0.022°C^{-1} for the highest conductivity value (i.e. 700 μS cm^{-1}). The 0.026°C^{-1} value is in agreement with values reported in the literature for rainwater with a similar mineral content (e.g. Bakalowicz, 1975). The final accuracy of our computation for NaCl mass balances was ±15%.

Comparison of hydrological and glaciological measurements

In Table 1, LF_n is expressed in mm w.e. year^{-1} (line 4 in Table 1) and $Q_{glacier}$ in L s^{-1} (line 7 in Table 1). On Antizana Glacier 15, values of LF_n and $Q_{glacier}$ were computed from 1995 to 2005. $Q_{glacier}$ values correspond to the possible annual contributions from the glacier to downstream runoff and range from 10.5 L s^{-1} in 1999 to 51.8 L s^{-1} in 1995 (Fig. 3). The lower values are those of La Niña years (1999 and 2000) when the glacier presented positive mass balances (Fig. 3). The higher values are those of El Niño events (1995, 1998, 2002–2003). Indeed, the mass balance is strongly dependent on the El Niño-Southern Oscillation as already shown by Francou *et al*. (2004).

Considering the decade 1995–2005, the mean LF_n value (1285 mm w.e. year^{-1}) is greater than the mean value of the precipitation input term (1020 mm w.e. year^{-1}). If all melt water contributes to runoff, the theoretical mean stream coefficient (LF_n/P_n) of the catchment corresponding to the glacierized area would be equal to 126% during this period. Assuming that precipitation is not underestimated in the higher parts of the glacier, this high value clearly indicates that the glaciers are retreating. When considering the whole catchment (1.37 km^2), the mean stream coefficient (Q_n/P_n) over 1997–2002 is much lower, i.e. 34%. Nevertheless, despite two years of positive mass balance during the period, this value is still higher than the values determined by precise hydrological analyses performed on the Pichincha volcano watershed close to Quito. On Pichincha Volcano, values were lower than 20% and indicated considerable infiltration when the soil was not saturated by rain events in the previous 24 hours (Perrin *et al*., 2001). Soils in high altitude areas of Ecuador generally generate very few surface streams (e.g. Perrin *et al*., 2001; Poulenard *et al*., 2001; Zehetener & Millar, 2006) and do not favour high stream coefficients.

Comparison of the melting term from the glacier $Q_{glacier}$ with discharge measurements Q_n over the 1997–2002 period are presented in Table 1 (lines 7 and 8) and Fig. 3. Over the 6-year study, the mean ratio between computed melting and discharge measurements was 1.5. Except in 1999, computed $Q_{glacier}$ values are always higher than Q_n values. In 2001 and 2002, $Q_{glacier}$ values are 2.3 times higher than Q_n values. In 1999 and 2000, when the glacier presented a positive net specific balance, $Q_{glacier}$ and Q_n values are similar. This indicates a stream deficit and shows that a considerable proportion of glacier melt does not reach Limni 15 station. To proceed with the estimation of this deficit, one has to estimate the evapotranspiration from the non-glacierized area.

The volumes of both evapotranspiration from the non-glacierized part and possible infiltration in glacierized and non-glacierized areas can be estimated using equation (2) for the period 1997–2002 (line 9, Table 1). Values range from 21 to 45 L s^{-1}, with a mean value of 32 L s^{-1}. The estimation of the ETR itself is difficult and only extreme values are thus considered, i.e. minimum and maximum estimates. The 1995–2005 mean sublimation on the Antizana Glacier 15 (362 mm year^{-1}) can be used as an approximate minimum value of the ETR in the non-glacierized area. The maximum value can be approximated using potential evapotranspiration (ETP) values from regional studies in Ecuador (Cadier & Pourrut, 1979; Le Goulven & Aleman, 1992; Bacci, 1997) and from measurements performed at slightly lower altitudes (4000 m a.s.l.) on the Antizana piedmont. Other studies performed on the Bolivian Altiplano (Vacher *et al*. 1994; Delclaux *et al*., 2007) above 3600 m a.s.l. also showed that the ETP decreases with altitude, mainly because of temperature decrease. Extrapolation of the results of these studies to the rarely-studied Antizana catchment enables rough estimation of the maximum value of the ETP of the order of

850 mm year^{-1}. Hence, although the actual values of annual ETR range from 362 to 850 mm year^{-1}, they are always lower than precipitation. Taking into account the two extreme estimations of ETR, the mean groundwater flow under glacierized and non-glacierized areas (Q_{gw} in equation (2)) would be between 25 and 16 L s^{-1} (lines 10 and 11, Table 1) for the 6-year period 1997–2002.

These figures of a possible groundwater flow ranging between 25 and 16 L s^{-1} are significant, considering the errors in estimating the other terms. Indeed, the error terms in accumulation (±400 mm w.e.) in the upper part of the glacier lead to an uncertainty as small as ±5 L s^{-1} in terms of flow. Moreover, the uncertainty in the measurement of discharge at Limni 15 station (Fig. 3) is much weaker than 16 or 25 L s^{-1}.

To analyse the hypothesis of infiltration flows more precisely, monthly values are now considered for the period from December 1996 to March 2003. Only the monthly melt volumes from the ablation area are used (see Favier, 2004, for details). The high density of ablation stakes enables precise ablation estimates in this area. The results show that for the last two years (2001–2002), when the discharge measurements were the most precise, the contribution of melt was clearly larger than that of runoff (Fig. 4).

Tracer experiments of subsuperficial flow

The results of the previous section corroborate the hypothesis of infiltration and groundwater flows that do not reach Limni 15 Station. In the present section, tracer experiments are analysed to determine whether infiltration occurs under the glacier or in the non-glacierized area.

The tracer experiments performed on the streams that cross the 1950 moraine showed that restitution ratios and transfer time values were linked to mean discharge values corresponding to the period of the experiment (Table 2, Fig. 5(a) and (b)). On one hand, the weaker the discharge, the later the restitution of the tracer occurred. Indeed, a higher flow implies a higher speed of the convective flow. On the other hand, the weaker the discharge, the lower the restitution ratio. This is typical of parallel slow and rapid circulations. The double porosity of the environment (micro-pores within the sand and macro-pores or spaces between rocks and ice blocks) may explain this behaviour since molecular diffusion in an environment with low porosity increases with a decrease in discharge. Another possible explanation is the presence of cryokarst (e.g. Hock, 2005) in the moraine. Indeed, during the flow of water in pipes, the thickness of the viscous sub-layer increases

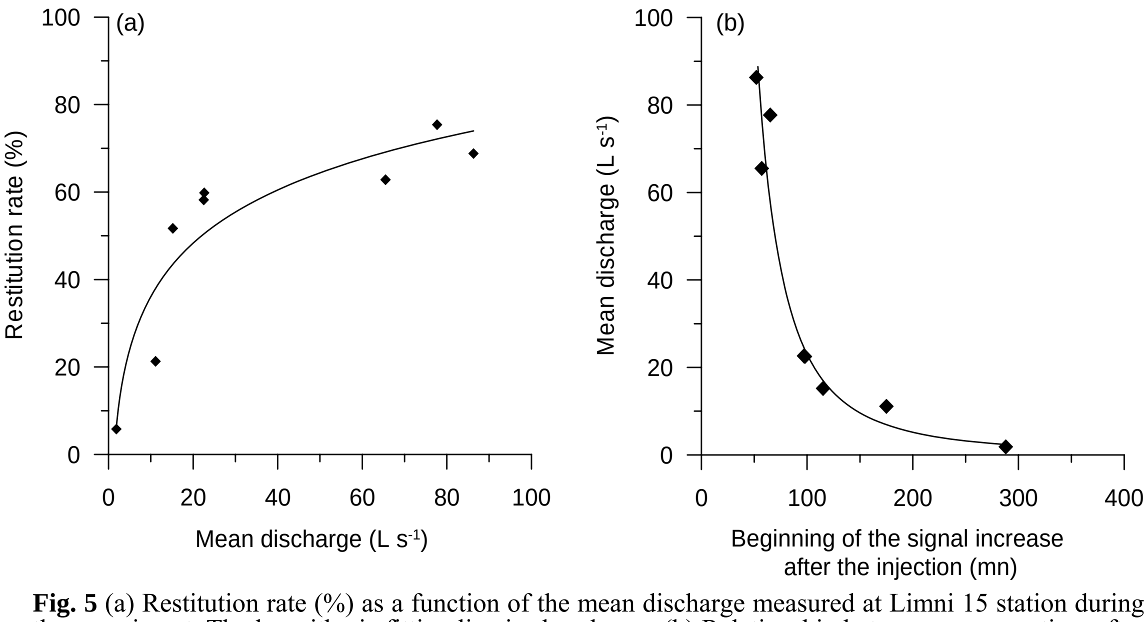

Fig. 5 (a) Restitution rate (%) as a function of the mean discharge measured at Limni 15 station during the experiment. The logarithmic fitting line is also shown. (b) Relationship between response time after injections and mean discharge. The power fitting line of the scatter of points is also shown.

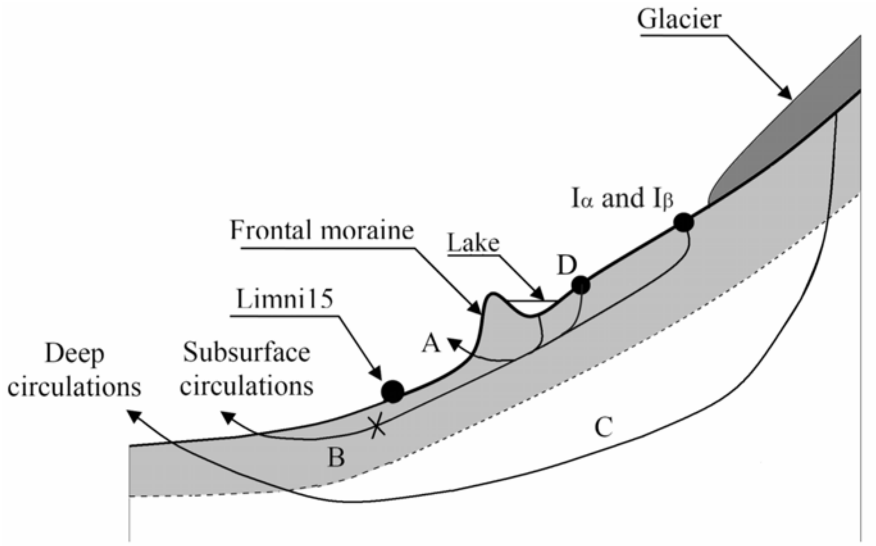

Fig. 6 Vertical cross-section along the axis of the glacier. Type A represents subsuperficial circulations that would flow out from the subsuperficial middle upstream from Limni 15 station. Type B corresponds to subsuperficial streams that would flow out downstream from Limni 15 station. Tracer experiments showed that infiltrations between point I_α (and I_β) and point D or at the level of the lake are fully retrieved at Limni 15 Station. Type C represents deep circulations.

with a decrease in velocity, promoting molecular diffusion to the viscous sub-layer in which the flow is slower (e.g. Bakalowicz, 2005). In both cases, the transfer of part of the tracer is delayed. Finally, the restitution ratio for the highest discharge was high (75%). Since part of the discharge entered slow flows (e.g. part of the surface stream entered the small lake located on the moraine; Fig. 2), such high values suggest that the discharge was conserved downstream of the moraine. As a consequence, water that infiltrated between point I_α (and I_β) and point D was retrieved at Limni 15 station (type A circulation in Fig. 6).

In the lake experiment, a brine solution containing m_i = 20.39 kg (±0.1%) of salt was injected into the small lake located on the moraine on 3 July 2003 at 14:00 h LT. The exponential decrease in the conductivity of the lake agreed well with a simple model of a reservoir with zero mineral load and an outlet discharge (Q_S) of water with tracer salt (C_S) (Ganino, 2003) (Fig. 2). This model allowed computation of a NaCl mass loss in the lake of 4.9 kg between 3 July at 14:00 h LT (injection time) and 5 July at 12:00 LT. This value was compared to the value obtained from interpretation of the measurements performed at the runoff gauging station. In order to estimate the contribution of lake water to river discharge, a simple mixing model (e.g. Collins, 1979) was applied considering that rapid flow of melt water through cryokarst and porous environments (with no tracer salt) mixed with the outflow from the lake (Q_S, C_S) (Fig. 2). Conductivity values measured at the gauging station revealed an increase in conductivity 7 h after injection (response time). Considering a time lag of 7 h, the mass of salt that transited at the station between 3 July at 21:00 h LT and 5 July at 19:00 h LT was 4.6 kg, i.e. a restitution rate of 93%. This experiment showed that infiltration at the level of the lake was completely retrieved at the runoff gauging station (type A circulation in Fig. 6). These two experiments indicate that type B groundwater flow can be excluded (Fig. 6).

Despite the uncertainty of the method, both experiments showed: first, that the surface streams flowing at the level of the glacier snout are fully accounted for at Limni 15 station (circulation type A, in Fig. 6); second, that missing runoffs were not due to infiltration toward the porous material of the moraine; and third, that the most likely hypothesis is that infiltration (Q_{gw}) occurs upstream from the glacier snout and below the ablation area, since melting occurs mainly in this area.

Possible interactions between groundwater flow and volcanic activity

Groundwater flows are common in volcanic areas and may have implications for the hydrothermal systems in the vicinity of the volcano (e.g. Violette *et al*., 1997). Some authors suggest that variations in groundwater flows have an impact on the stability of faults in volcanic areas (e.g. Saar & Manga, 2003) and enhance seismic activity. Infiltration of meteoric water (e.g. after heavy rainfall) may also enhance phreatic eruption activity, as reported for the Ecuadorian Pichincha stratovolcano (e.g. Smithsonian Institution, 2004), or for St Helens Mount (e.g. Mastin, 1994). Smith & McKibbin (1997) also argue that hydrothermal eruptions require pre-existence of a hydrothermal system. On Antizana, the occurrence of the serious flood on 20 August 1998 supports this hypothesis. The estimated discharge was 25 times larger than any other observation at the gauging station, and the water excavated a channel downstream from the glacier front. Although the sudden rupture of a water pocket has not been totally excluded, we suspect that the occurrence of groundwater outflow caused this flood. The extent of the groundwater flow under Antizana Glaciers could provide interesting elements to understand the significant seismic activity widely recorded on ice-covered volcanoes (e.g. Metaxian *et al*., 2003). This point is particularly interesting because the relationship between seismic activity and surface melting is still controversial as low frequency icequakes can be confused with long-period volcanic events (e.g. Metaxian *et al*., 2003). Such a relationship needs to be studied more thoroughly and Ecuadorian glaciers offer an excellent laboratory site for this task.

DISCUSSION AND CONCLUSIONS

Water from high altitude glaciers in the Antizana area is particularly valuable for human use due to its high potential energy and low rate of contamination. At the time of writing, glaciers represent an important water reserve whose volume is rapidly diminishing (Antizana Glacier 15 lost 36% and 23% of its surface over the 1956–2005 and 1993–2005 periods, respectively, Cáceres *et al*., 2005). Under climatic warming scenarios, the contribution of glacier melt may increase in the next 10 years but the reduction in glacier volume will finally have a progressive negative impact on melt water production and water contribution from glaciers. In Peru, Pouyaud *et al.* (2005) suggest that maximal water production from Cordillera Blanca glaciers would occur around 2050.

The present study on the Antizana Glacier 15 catchment showed that the theoretical stream coefficient of the glacierized area is high, with an interannual value of 126%, which reflects the present shrinkage of the glacier. During the study period, shrinkage was seen to accelerate during El Niño events, and to slow down in La Niña years. Considering the entire watershed, including glacierized and non-glacierized areas, the mean value of the annual stream coefficient is 34% for the period concerned (1997–2002). This low value, compared to the one of the glacierized area, is nevertheless higher than values measured in similar watersheds of the region that have no glaciers (Perrin *et al*., 2001). Since the stream coefficient value is currently weaker in non-glacierized areas than in glacierized areas, glacier shrinkage will have an impact on water supply and energy production and may require the use of security coefficients for the evaluation of water recollection projects that envisage using contributions from large glacierized areas.

Finally, it should be considered that groundwater flows may originate below the glacier and that these circulations must emerge downstream in the piedmont areas leading to stronger discharges than expected in several zones. The weak discharge values measured at the high altitude proglacial gauging station do not reflect the high rate of water production in glacierized areas and their contribution to low altitude discharges. One consequence of these processes is that the assessment of the contribution of the glacier to lower altitude discharges should include mass balance measurements, discharge measurements performed near the glacier fronts, and hydrological studies at a regional scale to enable complete estimation of the hydrological balance.

Acknowledgements The present study was supported by the Institut de Recherche pour le Développement (IRD, ex-ORSTOM) within scientific agreements with the INAMHI (Instituto Nacional de Meteorología e Hidrología) and the EMAAP-Q (Empresa Municipal de Alcantarillado y de Agua Potable de Quito) in Quito. Finally, we would like to extend our thanks to both the editor and two anonymous reviewers for their constructive remarks on this paper.

REFERENCES

Arck, M. & Scherer, D. (2002) Problems in the determination of sensible heat flux over snow. *Geografiska Annaler* **84A**(3/4), 157–169.

Bacci, J. (1997) Modelización hidropluviométrica del modelo global en un modelo distribuido: aplicación en la cuenca vertiente del Paute. Quito Ecuador: ORSTOM, *INAMHI, Série INSEQ* no. 19.

Bakalowicz, M. (1975) Variations de la conductivité d'une eau en fonction de la température, et précision des mesures. *Annales de Spéléologie* **30**(1), 3–6.

Bakalowicz, M. (2005) Karst groundwater: a challenge for new resources. *Hydrogeol. J.* **13**, 148–160.

Caballero, Y., Chevallier, P., Gallaire, R. & Pilco, R. (2004) Flow modelling in a high mountain valley equipped with hydropower plants: Rio Zongo Valley – Cordillera Real – Bolivia. *Hydrol. Processes* **18**, 939–957.

Cáceres, B., Maisincho, L., Taupin, J. D., Francou, B., Cadier, E., Delachaux, F., Bucher, R., Villacis, M., Paredes, D., Chazarin, J. P., Garces, A. & Laval, R.. (2005) Glaciares del Ecuador: Antizana y Carihuyarazo, balance de masa, topografía, meteorología & hidrología. *Informe del Año 2004.* IRD, EMAAP-Q, INAMHI Quito.

Cadier, E. & Pourrut, P. (1979) Inventaire et détermination des données nécessaires à l'utilisation rationnelle des ressources en eau dans le cadre d'une planification globale des ressources naturelles renouvelables. L'expérience de l'Equateur. *Cah. ORSTOM, série Hydrologie,* **XVI**(3-4), 171–211.

Cadier, E., Villacis, M., Garcés, A., Lhuissier, P., Maisincho, L., Laval, R., Paredes, D., Cáceres, B. & Francou, B. (2007) Melting modelling of a low latitude Andean glacier according to global and local climate variations: first results. In: *Glacier Mass Balance Changes and Meltwater Discharge* (ed. by P. Ginot & J.-E. Sicart), 66–74. (Proc. Foz do Iguaçu Symp. 2005). IAHS Publ. 318. IAHS Press, Wallingford, UK.

Collins, D. N. (1979) Quantitative determination of the subglacial hydrology of two alpine glaciers. *J. Glaciol.* **23**, 347–361.

Coudrain, A., Francou, B. & Kundzewicz, Z. W. (2005) Glacier shrinkage in the Andes and consequences for water resources—Editorial. *Hydrol. Sci. J.* **50**(6), 925–932.

Delclaux, F., Coudrain, A. & Condom, T. (2007) Evaporation estimation on Lake Titicaca: a synthesis review and modelling. *Hydrol. Processes* **21**(13), 1664–1677.

EMAAP-Q. (2002) Perfil del Proyecto de Agua potable Ríos Orientales. EMAAP report.

Favier, V. (2004) Etude du bilan d'énergie de surface et de la production des écoulements de fonte d'un glacier des Andes d'Equateur; relation glacier–climat en zone tropicale. PhD Thesis, Université de Montpellier II, France.

Favier, V., Wagnon, P. & Ribstein, P. (2004a) Glaciers of the outer and inner tropics: A different behaviour but a common response to climatic forcing. *Geophys. Res. Lett.* **31**, L16403.

Favier, V., Wagnon, P., Chazarin, J. P., Maisincho, L. & Coudrain, C. (2004b) One-year measurements of surface heat budget on the ablation zone of Antizana Glacier 15, Ecuadorian Andes. *J. Geophys. Res.* **109**(D18), D18105.

Fountain, A. & Tangborn, W. (1985) The effect of glaciers on streamflow variations. *Water Resour. Res.* **21**, 579–586.

Francou, B., Ramírez, E., Cáceres, B. & Mendoza, J. (2000) Glacier Evolution in the Tropical Andes during the last decades of the 20th century: Chacaltaya, Bolivia, and Antizana, Ecuador. *Ambio* **29**, 416–422.

Francou, B. & Pouyaud, B. (2004) Método de observación de glaciares en los Andes tropicales. mediciones de terreno y procesamiento de datos. IRD GREAT ICE – Report.

Francou, B., Vuille, M., Favier, V. & Cáceres, B. (2004) New evidence for an ENSO impact on low-latitude glaciers: Antizana Glacier 15, Andes of Ecuador, 0°28′S. *J. Geophys. Res.* **109**(D18), D18106.

Ganino, C. (2003) Hydrologie des glaciers 15 et Crespo de l'Antizana (Equateur). MSc Thesis, Magistère des sciences de la Terre et de l'Univers, ENS, Lyon, France.

Hastenrath, S. (1981) *The Glaciation of the Ecuadorian Andes.* Balkema, The Netherlands.

Hock, R. (2005) Glacier melt: A review of processes and their modelling. *Progr. Phys. Geogr.* **29**(3), 362–391.

Kaser, G. (2001) Glacier–climate interaction at low-latitudes. *J. Glaciol.* **47**(157), 195–204.

Kaser, G. & Osmaston, H. A. (2002) *Tropical Glaciers*. Cambridge University Press, New York, USA.

Kaser, G., Juen, I., Georges, C., Gomez, J. & Tamayo, W. (2003a) The impact of glaciers on the runoff and the reconstruction of mass balance history from hydrological data in the tropical Cordillera Blanca, Perú. *J. Hydrol.* **282**, 130–144.

Kaser, G., Fountain, A. & Jansson, P. (2003b) A manual for monitoring the mass balance of mountain glaciers – with particular attention to low latitude characteristics. Technical Documents in Hydrology, UNESCO-PHI.

Lecce, S. A. (1993) Flow separation and diurnal variability in the hydrology of Conness Glacier, Sierra Nevada, California, USA. *J. Glaciol.* **39**, 216–222.

Le Goulven, P. & Aleman, M. (1992) Regionalización climática (lluvia y ETP) en los Andes del Ecuador, Metodología, resultados y aplicaciones. In: VIIIavos Días Hidrológicos "Regionalización en Hidrología – Aplicación al Desarrollo". ORSTOM, Montpellier, 22–23/9/1992.

Mastin, L. G. (1994) Explosive tephra emissions at Mount St. Helens, 1989–1991: The violent escape of magmatic gas following storms? *Geophys. Soc. Am. Bull.* **106**, 175–185.

Métaxian, J. P., Araujo, S., Mora, M. & Lesage, P. (2003) Seismicity related to the glacier of Cotopaxi volcano, Ecuador. *Geophys. Res. Lett.* **30**(9), 1483 doi:10.1029/2002GL016773.

Perrin, J. L., Bouvier, C., Janeau, J. L., Ménez, G. & Cruz, F. (2001) Rainfall/runoff processes in a small peri-urban catchment in the Andes mountains. The Rumihurcu Quebrada, Quito (Ecuador). *Hydrol. Processes* **15**, 843–854. doi:10.1002/hyp.190.

Poulenard, J., Podwojewski, P., Janeau, J. L. & Collinet, J. (2001) Runoff and soil erosion under rainfall simulation of Andisols from the Ecuadorian Páramo: effect of tillage and burning. *Catena* **45**, 185–207.

Pouyaud, B., Zapata, M., Yerren, J., Gomez, J., Rosas, G., Suarez, W. & Ribstein, P. (2005) Avenir des ressources en eau glaciaire de la Cordillère Blanche. *Hydrol. Sci. J.* **50**(6), 999–1022.

Ribstein, P., Tiriau, E., Francou, B. & Saravia, R. (1995) Tropical climate and glacier hydrology: A case study in Bolivia. *J. Hydrol.* **165**, 221–234.

Saar, M. O. & Manga, M., Seismicity induced by seasonal groundwater recharge at Mt. Hood, Oregon. *Earth & Planetary Science Letters* **214**, 605–618.

Sicart, J. E., Wagnon, P. & Ribstein, P. (2005) Atmospheric controls of the heat balance of Zongo Glacier (16°S, Bolivia). *J. Geophys. Res.* **110**, D12106, doi:10.1029/2004JD005732.

Sicart, J. E., Ribstein, P., Francou, B., Pouyaud, B. & Condom, T. (2007) Glacier mass balance of tropical Zongo glacier, Bolivia, comparing hydrological and glaciological methods. *Global and Planetary Change* **59**(1), 27–36.

Sigg, L., Stumm, W. & Behra, P. (1992) *Chimie des Milieux Aquatiques*. Masson, France.

Smith, T. A. & McKibbin, R. (1997) Modelling of hydrothermal eruptions: a review. In: *Proc. 19th NZ Geothermal Workshop*, 123–128.

Smithsonian Institution. (2004) Guagua Pichincha (Ecuador): Phreatic explosions in November 2001 and October-December 2002. *Bulletin of the Global Volcanism Network* 29(6).

Vacher, J., Imana, E. & Canqui, E.(1994) Las caracteristicas radiativas y la evapotranspiracion potencial en el Altiplano boliviano. *Revista de Agricultura (BOL)* **50**(24), 4–11. http://horizon.documentation.ird.fr/exl-doc/pleins_textes/pleins_textes_7/b_fdi_03_01/41712.pdf.

Violette, S., Ledoux, E., Goblet, P. & Carbonnel, J. P. (1997) Hydrologic and thermal modeling of an active volcano: the Piton de la Fournaise, Reunion. *J. Hydrol.* **191**, 37–63.

Wagnon, P., Ribstein, P., Francou, B. & Pouyaud, B. (1999) Annual cycle of energy balance of Zongo Glacier, Cordillera Real, Bolivia. *J. Geophys. Res.* **104**(D4), 3907–3923.

Zehetner, F. & Miller, P. M. (2006) Erodibility and runoff-infiltration characteristics of volcanic ash soils along an altitudinal climosequence in the Ecuadorian Andes. *Catena* **65**, 201–213.

Received 16 November 2006; accepted 17 September 2007